ELSEVIER

International Journal of Refractory Metals & Hard Materials 16 (1998) 343–352

International Journal of
REFRACTORY METALS
& HARD MATERIALS

Formation of mullite coatings on silicon-based ceramics by chemical vapor deposition

S. N. Basu, Ping Hou, V. K. Sarin

Manufacturing Engineering Department, Boston University, Boston, MA02215, USA

Received 9 March 1998; accepted 16 August 1998

Abstract

Dense, uniform, mullite coatings have been deposited by chemical vapor deposition on SiC substrates, using a $AlCl_3$–$SiCl_4$–CO_2–H_2 system. The typical coating microstructure consisted of a thin layer of nanocrystallites of γ-Al_2O_3 in vitreous silica at the coating–substrate interface, with columnar mullite grains over this interfacial layer. The composition of the coating was graded such that the outer surface of the coating was highly alumina rich. The changes in the coating microstructure with processing parameters are discussed. The ability of mullite to incorporate such large composition variations is discussed in the light of vacancy formation as the Al/Si ratio is increased, and the ordering of these vacancies leads to changes in lattice parameters. The formation of domains was studied by measuring the spacing of superlattice spots in electron diffraction patterns, and the relationship between domain size and Al/Si ratio is discussed.

Keywords: Mullite coatings; Chemical vapor deposition; Lattice parameters

1. Introduction

Silicon-based ceramics such as SiC and Si_3N_4 have excellent potential for widespread use in high temperature applications such as heat exchangers, gas turbines and internal combustion engines. Although these ceramics have high strength, high thermal conductivity, low coefficient of thermal expansion (CTE) and excellent high temperature stability and oxidation resistance, they are susceptible to high temperature corrosion and contact stress damage [1]. It has long been established that protective coatings on Si-based ceramics are the desired solution to overcome these problems. Mullite ($3Al_2O_3{\cdot}SiO_2$) is an excellent candidate material for such coatings due to its excellent creep and thermal shock resistance, as well as excellent chemical stability, strength and oxidation and corrosion resistance at elevated temperatures [2]. Additionally, mullite has an excellent CTE match with SiC.

Deposition of mullite coatings by plasma spraying has been reported in the literature [3]. However, these coatings exhibited problems of non-uniformity and the presence of microcracks, which are characteristic of the plasma spraying process. The Materials Group at Boston University has been involved in growing mullite coatings by chemical vapor deposition (CVD). CVD is an ideal technique to grow dense coatings on complex shapes at temperatures far below the melting point of the substrates. This paper presents some of the results of this ongoing research.

2. Experimental details

Mullite coatings were grown in a CVD reactor from the $AlCl_3$–$SiCl_4$–CO_2–H_2 system in which the overall reaction of mullite formation is given as:

$$6AlCl_3+2SiCl_4+13CO_2+13H_2 = 3Al_2O_3{\cdot}2SiO_2 + 13CO+26HCl \quad (1)$$

The depositions were carried out at 950°C, with a total pressure of 75 Torr. The input Al/Si ratios were varied among 1, 2, 3 and 4 by changing the relative input partial pressures of $SiCl_4$ or $AlCl_3$ but keeping the total metal chloride partial pressure fixed at 0.53 Torr.

The coatings were examined by X-ray diffraction analysis (XRD) and by scanning electron microscopy (SEM). Electron transparent specimens of the coatings

0263-4368/98/$ — see front matter
PII: S0263-4368(98)00043-2

were made in cross-section and the samples were examined using a JEOL 2010 transmission electron microscope (TEM). Compositional analysis of the coatings was carried out by energy dispersive spectroscopy (EDS) in a VG HB603 dedicated scanning transmission electron microscope (STEM) using a 4 nm electron proble.

3. Results and discussion

Mullite is typically formed by a high temperature reaction between an alumina–silica interface. The first attempts at growing mullite coatings on SiC at Boston University involved the growth of micron thick alternating layers of alumina and silica by CVD, followed by a high temperature anneal to facilitate mullite formation. We found that the reaction rate was very slow at the interface and, on cooling, the unreacted silica crystallized and fractured on thermal cycling, leading to coating spallation [4]. Such a fracture in the crystallized silica layer is shown in Fig. 1. It was therefore necessary to deposit alumina and silica directly as mullite or on a much finer scale to facilitate rapid mullite formation on annealing.

Detailed thermodynamic analysis of the $AlCl_3$–$SiCl_4$–CO_2–H_2 system was carried out to identify the parameters to be used for CVD mullite growth [5]. CVD ternary phase diagrams were constructed between $AlCl_3$, $SiCl_4$ and CO_2 for various partial pressures of H_2. In addition, the deposition efficiency (fraction of Al and Si in the input chlorides ending up as mullite) of mullite was also calculated under different conditions. Figure 2 shows a CVD binary phase diagram of the $AlCl_3$–$SiCl_4$–CO_2–H_2 system at 1000°C and 75 Torr of total pressure. As expected, mullite is formed when the ratio of Al/Si in the input chlorides is at the stoichiometric value of 3. However, the fact that mullite is not a line compound of fixed stoichiometry allows for mullite to be thermodynamically stable over a larger range of input conditions as shown by the shaded region in the figure. As can be seen in Fig. 2, low chloride concentrations need to be used to obtain C-free deposits. Fortunately, these conditions also correspond to higher deposition efficiencies, indicating that high input concentrations of CO_2 should be used.

Mullite coatings were successfully grown on SiC by CVD over a wide range of input conditions. The growth temperature and total pressure were found to be optimum at 950°C and 75 Torr, and the Al/Si ratio in the input chlorides was varied from 1 to 4. Figure 3 shows a typical dense, adherent and uniform mullite coating on SiC. Figure 4 shows the X-ray diffraction pattern of the coating, where all non-substrate peaks match closely with mullite. One interesting feature of the XRD pattern is the presence of a strong (001) texturing in the coating. The (001) peak intensity, which has a relative intensity of 20 in non-textured mullite, is actually more intense than the (120)/(210) peak which should have a relative intensity of 100. Since it is known that mullite crystallites grow preferentially in the (001) direction, such an orientation with the growth direction is not surprising.

Figure 5 shows a TEM bright-field micrograph of a typical mullite coating on SiC in cross-section. The figure shows that the coating has two distinct layers. Most of the coating consists of columnar crystallite

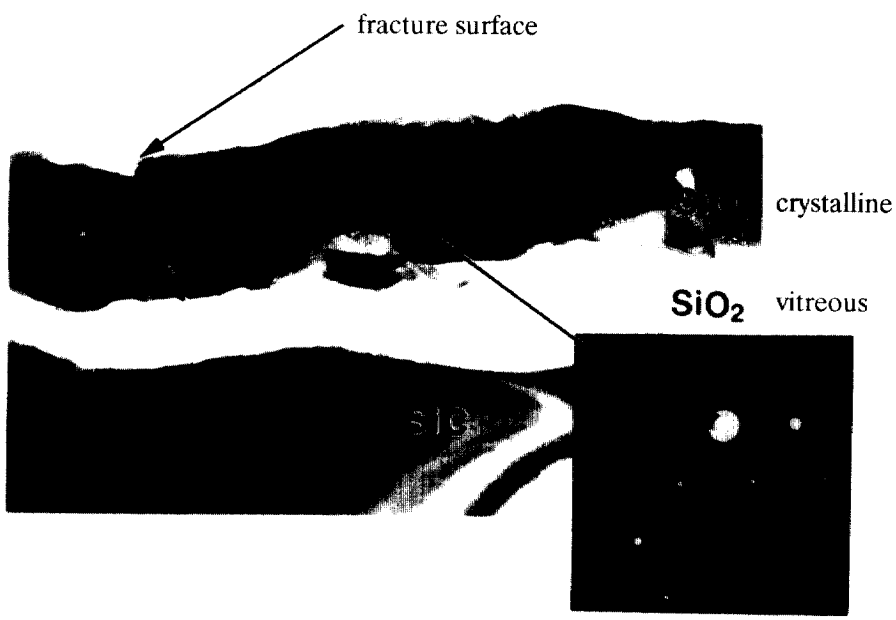

Fig. 1. Spallation of multilayered alumina/silica coatings, due to crystallization of silica on annealing.

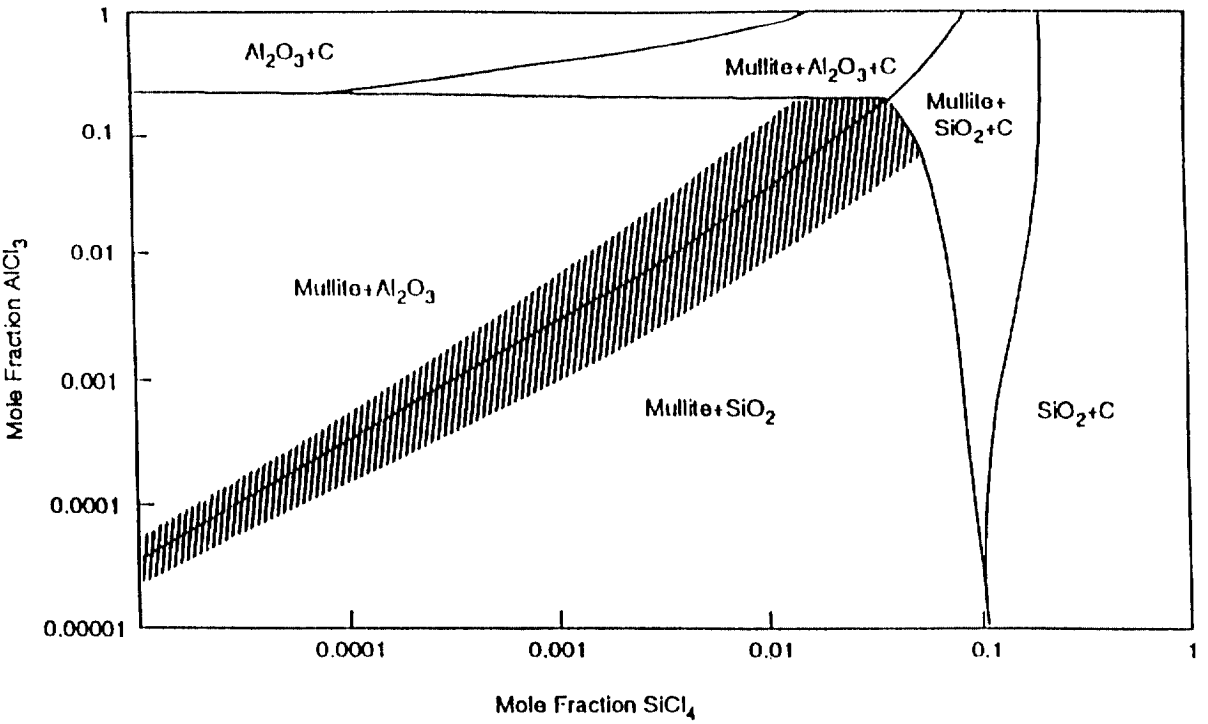

Fig. 2. CVD binary phase diagram of the $AlCl_3$–$SiCl_4$–CO_2–H_2 system at 1000°C and 75 Torr total pressure.

grains. The inset electron diffraction pattern clearly identifies these grains as mullite. Diffraction patterns from various zone axes were taken from these grains [6], and they were all consistent with mullite. At the interface between the coating and substrate, another distinct layer is present, that appears non-crystalline. Figure 6 shows a higher magnification TEM bright-field micrograph of this region. However, the inset diffraction pattern from this region in Fig. 6 shows the presence of rings, implying that nanocrystallites are present, probably within a vitreous matrix. The ring diffraction pattern from these crystallites matched very well with γ-Al_2O_3. The matrix was found to be Si-rich by analysis in the STEM, and is essentially vitreous silica with perhaps some Al dissolved in it. Due to the very fine size and relatively dense packing of the γ-Al_2O_3 crystallites, it was difficult to ensure that only the matrix contributed to the signal. Thus, it is unclear whether the small Al signal from the vitreous matrix was due to dissolved Al in the matrix or from an imbedded γ-Al_2O_3 precipitate.

Fig. 3. SEM image of dense, adherent and uniform mullite coating on SiC.

Figure 7 shows a variation of Al/Si ratios across the nanocrystalline region and the mullite grains, measured in the STEM using a 4 nm electron probe. The figure shows the composition at the coating/substrate interface to be less than that of stoichiometric mullite (Al/Si ratio of 3), with the Al/Si ratio increasing steadily until the coating surface is highly Al-rich. Mullite grains appear to nucleate from the nanocrystalline region when the Al/Si ratio at the nanocrystalline/columnar interface at which mullite nucleates was found to average 3.24 for coatings grown under a variety of conditions. The presence of a critical concentration of Al/Si is consistent with reports in the literature on the studies of mullite formation by heating finely mixed Al_2O_3 or SiO_2 [7].

The thickness of the nanocrystalline region can be controlled by changing the processing parameters and the substrate material. The thickness of the nanocrystalline layer on SiC substrates, as the input Al/Si ratio

(in the form of chlorides) was varied among 1, 2, 3 and 4, is plotted in Fig. 8. It can be seen that increasing the input Al/Si ratio decreases the nanocrystalline layer thickness, presumably because the critical Al/Si ratio for mullite nucleation occurs faster. Mullite coatings grown on mullite substrates using an input Al/Si ratio of 3 show no nanocrystalline layer, and the presence of very fine mullite grains right at the coating/substrate interface, due to the easy nucleation of mullite on mullite.

The input Al/Si ratios also affected the growth rates of the coatings. In all cases, the total metal chloride partial pressure (sum of partial pressures of $SiCl_4$ or $AlCl_3$) was fixed at 0.53 Torr. Figure 9 shows the variation of growth rate with input composition and its comparison with pure Al_2O_3 and SiO_2. The figure shows that the growth rate when either the $SiCl_4$ or $AlCl_3$ is cut off to grow pure Al_2O_3 or SiO_2, is slower than when both species are input. Also, the growth rates of off-stoichiometric Al/Si input ratios of 1, 2 and 4 are pretty much the same, while the growth rates are fastest when the Al/Si input ratio is held at the stoichiometric value of 3. Another interesting feature was that the 3:1 coatings showed the most pronounced (001) texture.

When the mullite coatings grown on SiC substrates were annealed at 1200°C for 100 h, the nanocrystalline region transformed into mullite. Figure 10 shows crystallites of mullite in the nanocrystalline region formed after annealing. The longer dimension of these crystallites is along the *c*-axis, the preferred growth direction of mullite. It is important to note that, eventually, the entire nanocrystalline layer can transform into mullite without any cracking or adverse effects on the adhesion of the coating.

The gradation of the composition from being Si-rich (compared to stoichiometric mullite) at the coating/substrate interface to highly Al-rich at the outer coating surface has several advantages. Firstly, the presence of a native silica layer on the surface of SiC substrates assures good adhesion of the coating. Preliminary thermal cycling tests indicate that the mullite coatings have excellent adhesion. On the other hand, Al/Si ratios as high as 8 have been found at the

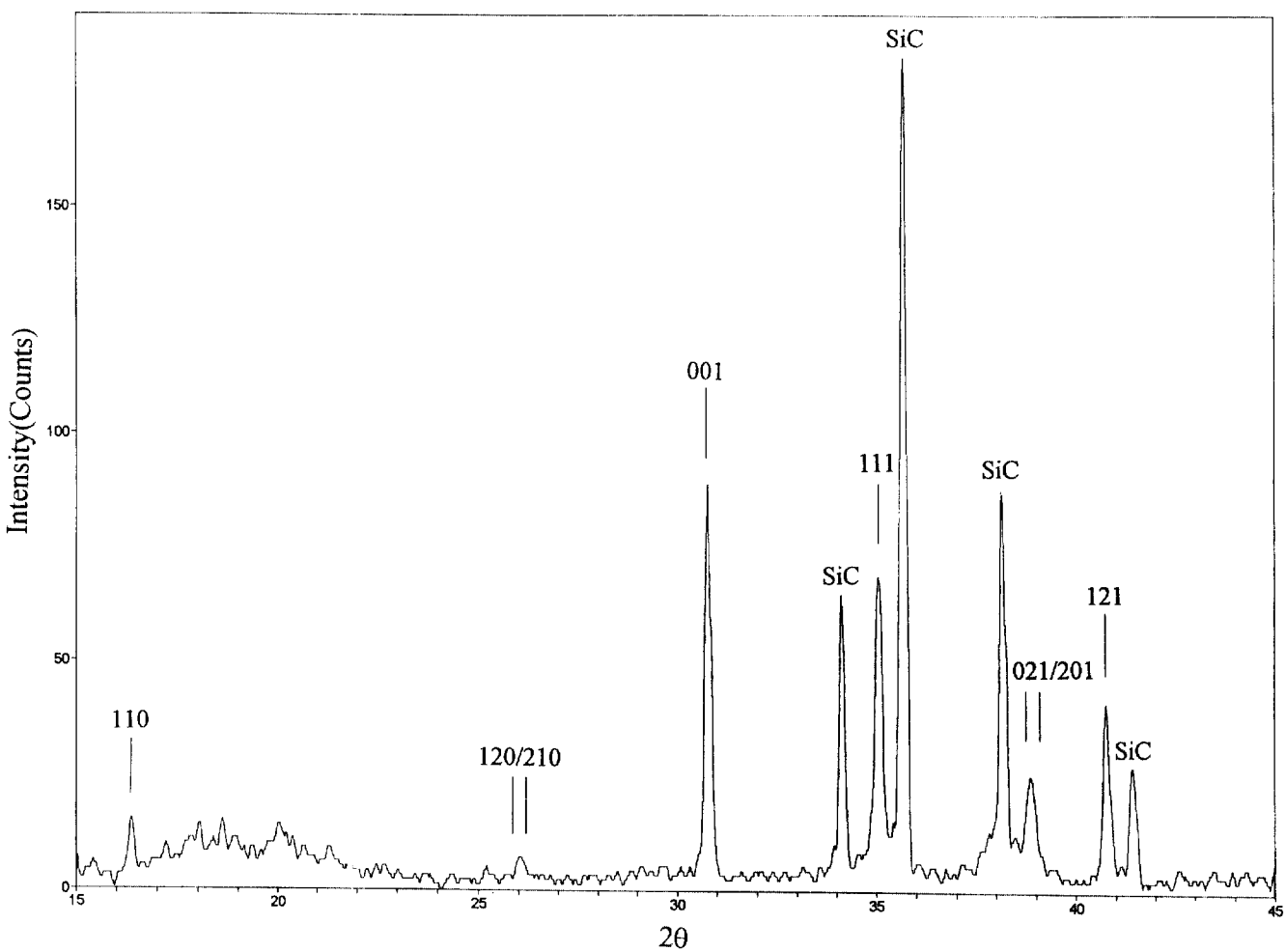

Fig. 4. XRD plot of mullite coating, showing strong (001) texturing.

coating surface, which is among the highest Al/Si ratios found in mullite structures. This high Al content is responsible for the coatings having excellent hot corrosion properties. The results of the excellent performance of these coatings in the presence of molten salts on the coating surface, and in a modified burner jet rig test, are presented elsewhere [8]. The gradation of the composition, and therefore its properties, also presumably reduce residual stresses on thermal cycling arising from CTE mismatch between the coating and substrate. Another interesting implication is that we have a high Al content in a mullite structure. Presumably, if the Al/Si ratio was raised further, it is possible to approach an alumina with the mullite structure, which should be able to incorporate plastic deformation without fracture better than the corundum structure which does not have active slip systems perpendicular to the basal plane.

We will now address briefly how mullite can incorporate such a large variation in composition without altering its structure. The subject has been discussed in detail elsewhere [9]. Mullite is a defect structure of sillimanite ($Al_2O_3 \cdot SiO_2$), in which some of the Si^{4+} ions are substituted by Al^{3+} ions by the following reaction:

$$2Si^{4+} + O^{2} \Leftrightarrow 2Al^{3+} + \square \tag{2}$$

where $\square$ is an oxygen vacancy. Thus the number of oxygen vacancies in a unit cell, x, is related to the Al/Si ratio as:

$$x = \frac{\left(\frac{Al}{Si} - 2\right)}{\left(\frac{Al}{Si} + 1\right)} \tag{3}$$

In fact, mullite can be written as:

$$Al_2^{VI}(Al_{2+2x}^{IV}Si_{2-2x}^{IV})O_{10-x} \tag{4}$$

where IV and VI are the coordination states of the cations. The presence of the oxygen vacancies causes

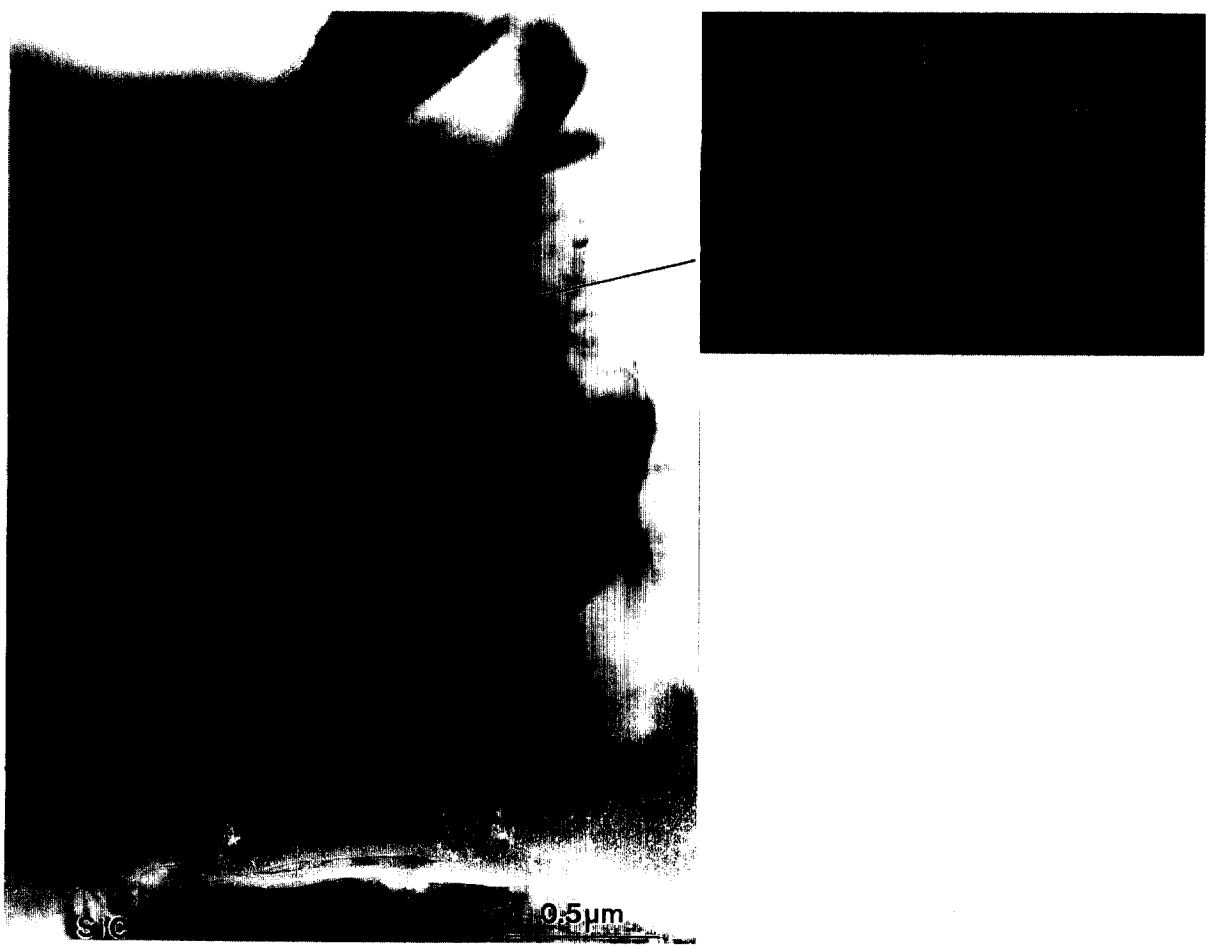

Fig. 5. TEM bright-field micrograph of a mullite coating on SiC in cross-section showing two distinct layers. The diffraction pattern from the oclumnar grains is consistent with the [010] diffraction pattern of mullite. Pairs of superlattice spots, spaced 2S apart, are seen aligned in the a^* direction.

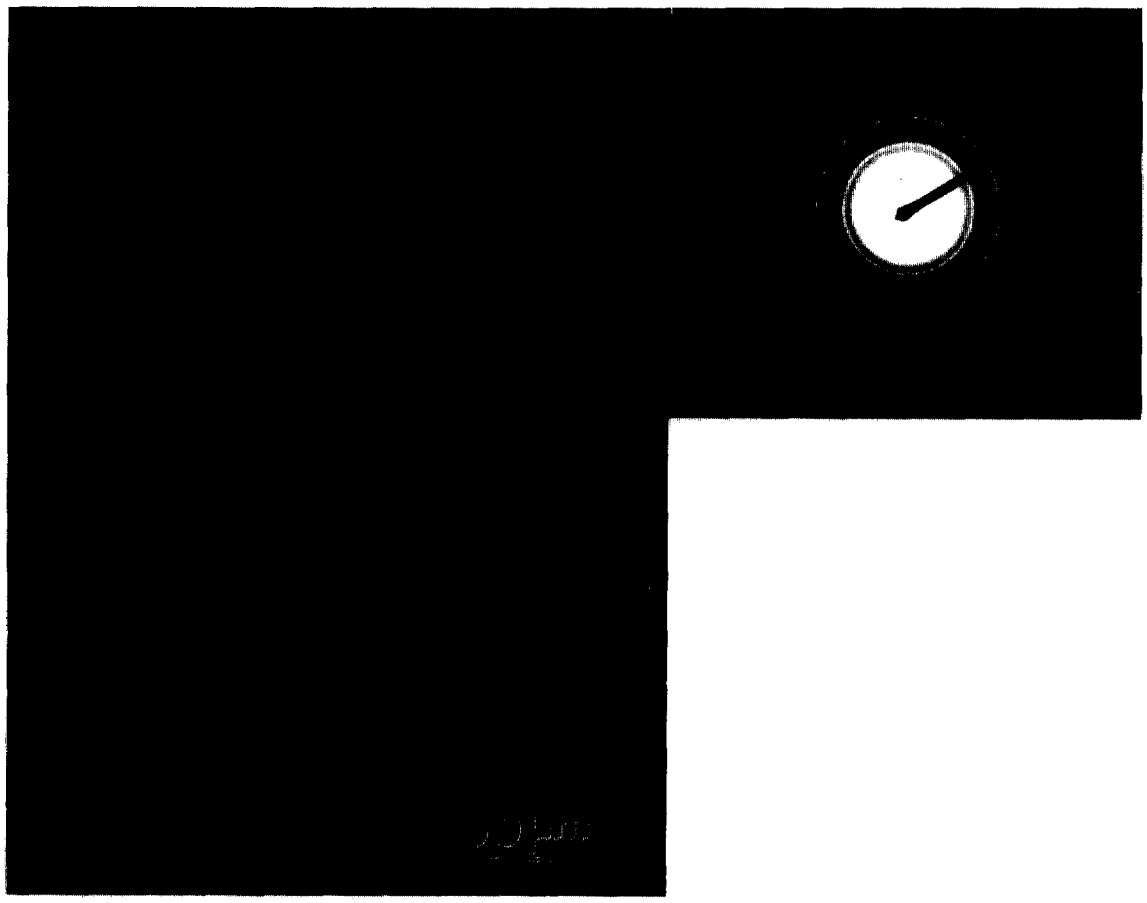

Fig. 6. TEM bright-field micrograph of the nanocrystalline region with inset diffraction pattern. The spacing of the rings identifies the nanocrystallites to be γ-Al_2O_3.

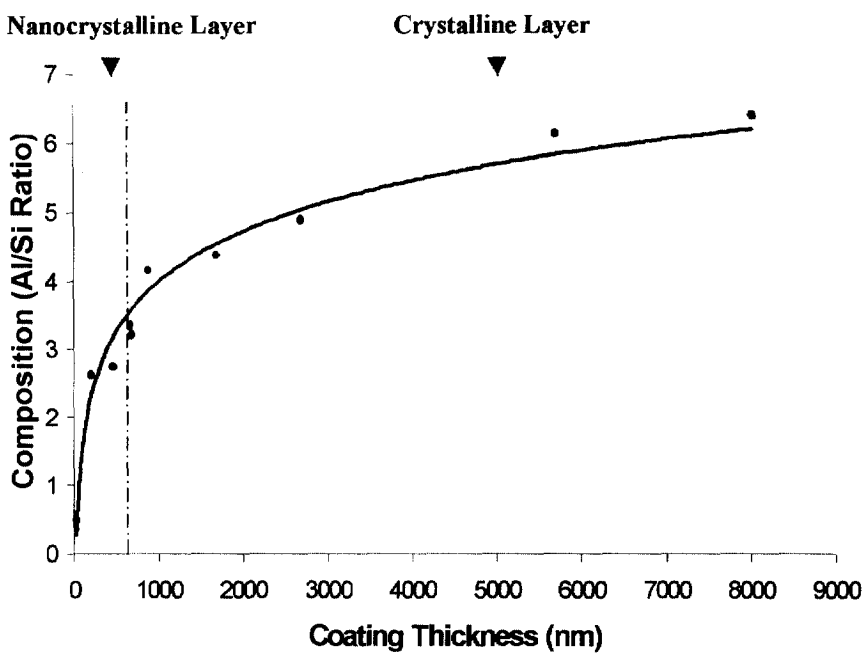

Fig. 7. Variation of Al/Si ratios across the nanocrystalline region and the mullite grains.

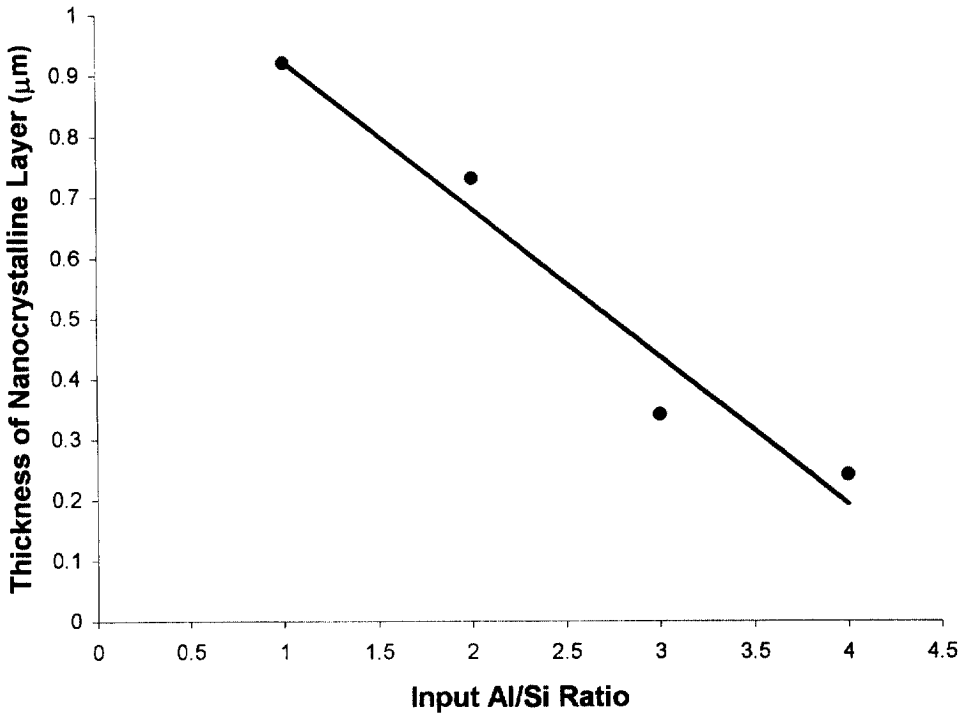

Fig. 8. Plot of thickness of the nanocrystalline layer on SiC substrates, as the input Al/Si ratio was varied among 1, 2, 3 and 4, showing a linear dependency.

the Al^{3+} and Si^{4+} ions, which are ordered on the (00z) planes in sillimanite, to disorder, thus reducing the lattice parameter c of mullite to half the value of sillimanite. At high Al/Si contents, the oxygen vacancies order to minimize the free energy of the crystal. In addition to the short range ordering of vacancies, long range 2-D compositions have been reported in mullite [10]. These modulations give rise to domains separated by anti-phase domain boundaries (APB) oriented parallel to (001) planes [11]. These domains produce superlattice spots in the [010] diffraction pattern of mullite. Figure 5 shows pairs of these superlattice spots oriented along the a^* direction.

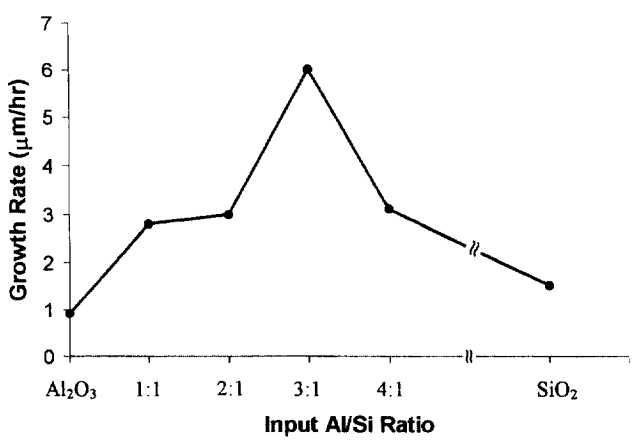

Fig. 9. Plot of variation of growth rate with input composition and its comparison with growth rate of pure Al_2O_3 and SiO_2.

The spacing between the superlattice spots, $2S$, is related to the domain size. Cameron plotted the parameter S/a as a function of the parameter x, which is an increasing function of the Al/Si ratio [10]. Figure 11 shows this plot (Cameron's data is marked by '+'), where at low values of x, S/a decreases linearly. However, beyond $x = 0.47$, the plot indicates that a constant value of S/a is approached. This means that at larger Al/Si ratios, as the vacancy concentrations become very high, more and more diffusion is required to form larger and larger domains. We measured the spacing between the superlattice spots as a function of Al/Si ratios in our coatings. When we plotted our data on Cameron's plot (marked as 'o' in Fig. 11), it is seen that the linear region was extended to much higher values of x. This implies that we get much larger domain sizes in our Al-rich portions of coatings as compared to those found by Cameron in samples formed by diffusing Al_2O_3 and SiO_2 powders at high temperatures. The explanation is that in our CVD process, surface diffusion occurs rapidly as the coatings grow, thereby allowing longer range composition modulations as compared to that followed by slower bulk diffusion in Cameron's case.

Another interesting implication of going to higher Al/Si ratios is the change in lattice parameters with

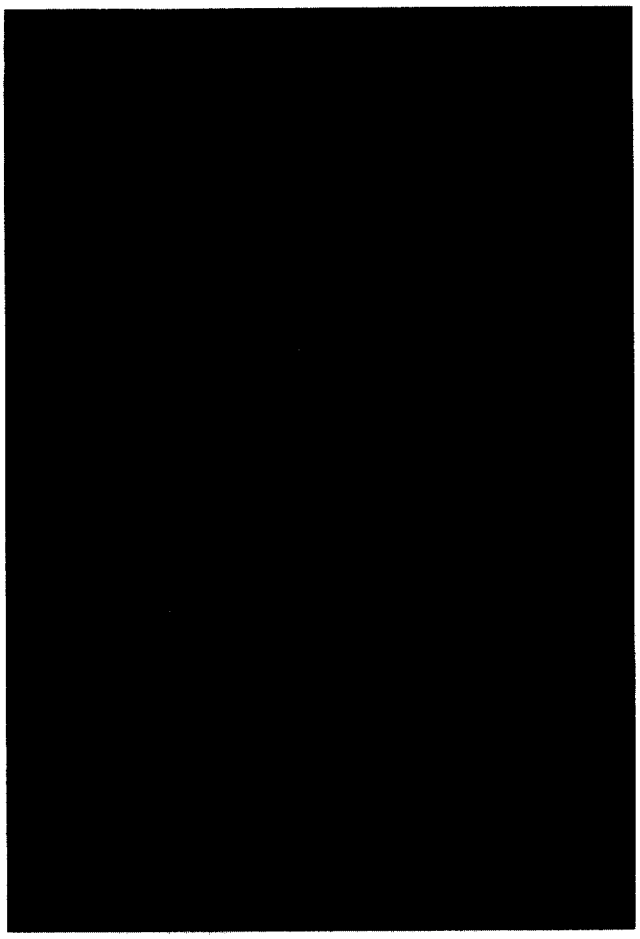

Fig. 10. Formation of mullite crystallites in the nanocrystalline region formed after annealing for 100 h at 1200°C.

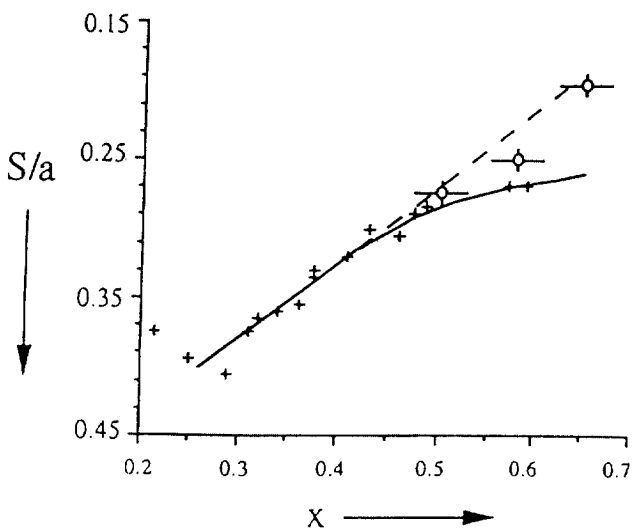

Fig. 11. Variation of parameter S/a with oxygen vacancy concentration (x). Cameron's data [10] are marked by '+' and data from this study are marked by 'o'. Our data fits well with the linear extrapolation of Cameron's data at low values of x.

($a = 0.7546$, $b = 0.7690$ and $c = 0.288$ nm), with the b lattice parameter being slightly larger than a. As the Al/Si ratio increases, leading to an increase in the oxygen vacancy concentration, these vacancies tend to line up preferentially along the b-axis, thereby effect ively reducing the b lattice parameter and increasing the a lattice parameter. We thus found that the mullite structure goes from orthorhombic to tetragonal as we go from the interface to the outer surface of the coating. This preferential vacancy ordering has another interesting implication. As deposited mullite coatings often show no splitting of the (120)/(210) peaks in XRD plots, implying a tetragonal structure; Figure 12(a) shows such a plot. On annealing, the structure transforms to orthorhombic, showing a clear splitting of the (120)/(210) peaks as shown in Fig. 12(b). This may be due to the fact that the formation of the mullite crystal from a vapor phase is so highly non-equilibrium that it leads to the formation of a high supersaturation of defects such as oxygen vacancies. Such high vacancy concentrations can only be stabilized by ordering along the b-axis. On annealing, the extra vacancies are annealed out, and a much lower equilibrium vacancy concentration is reached. This causes the structure to revert back to its original orthorhombic unit cell.

4. Conclusions

Dense, adherent mullite coatings have been deposited on SiC substrates by a CVD process. The coatings are compositionally graded, with the Al/Si ratio being relatively low at the interface and increasing to values as high as 8 towards the outer surface of the coating. This compositional gradation led the coatings to exhibit excellent adhesion and hot corrosion resistance. Under most circumstances, the coating starts off as an intimate mixture of nanocrystalline γ-Al_2O_3 in a vitreous silica matrix. When a critical Al/Si ratio is reached, mullite grains nucleate and grow in a columnar fashion, typically with the c-axis corresponding to the growth direction, leading to a (001) texture. The thickness of the nanocrystalline layer can be reduced by increasing the input Al/Si ratio. However, the growth rate of the coatings was found to be fastest when the stoichiometric Al/Si ratio of 3 was used. On annealing, the nanocrystalline region transformed into mullite, accompanied by a conversion of the structure from tetragonal to orthorhombic.

The structure of the Al-rich mullite grains was studied by electron diffraction. The structure converted from orthorhombic to tetragonal as the Al/Si ratio was increased, due to the ordering of oxygen vacancies along the b-axis. In addition, superlattice spots were seen in the [010] diffraction pattern of mullite,

indicating the formation of domains. The spacing between the superlattice spots decreased with increasing Al/Si ratios, indicating an increase in domain sizes. Some of the largest domain sizes ever reported were found in this study, and are attributed to a better atom mobility by surface diffusion during coating growth.

Acknowledgements

This research is sponsored by the US Department of Energy, Assistant Secretary for Energy Efficiency, Office of Transportation Technologies, as part of the Ceramics Technology Project of the Propulsion System Materials Program and Fossil Energy AR and TD

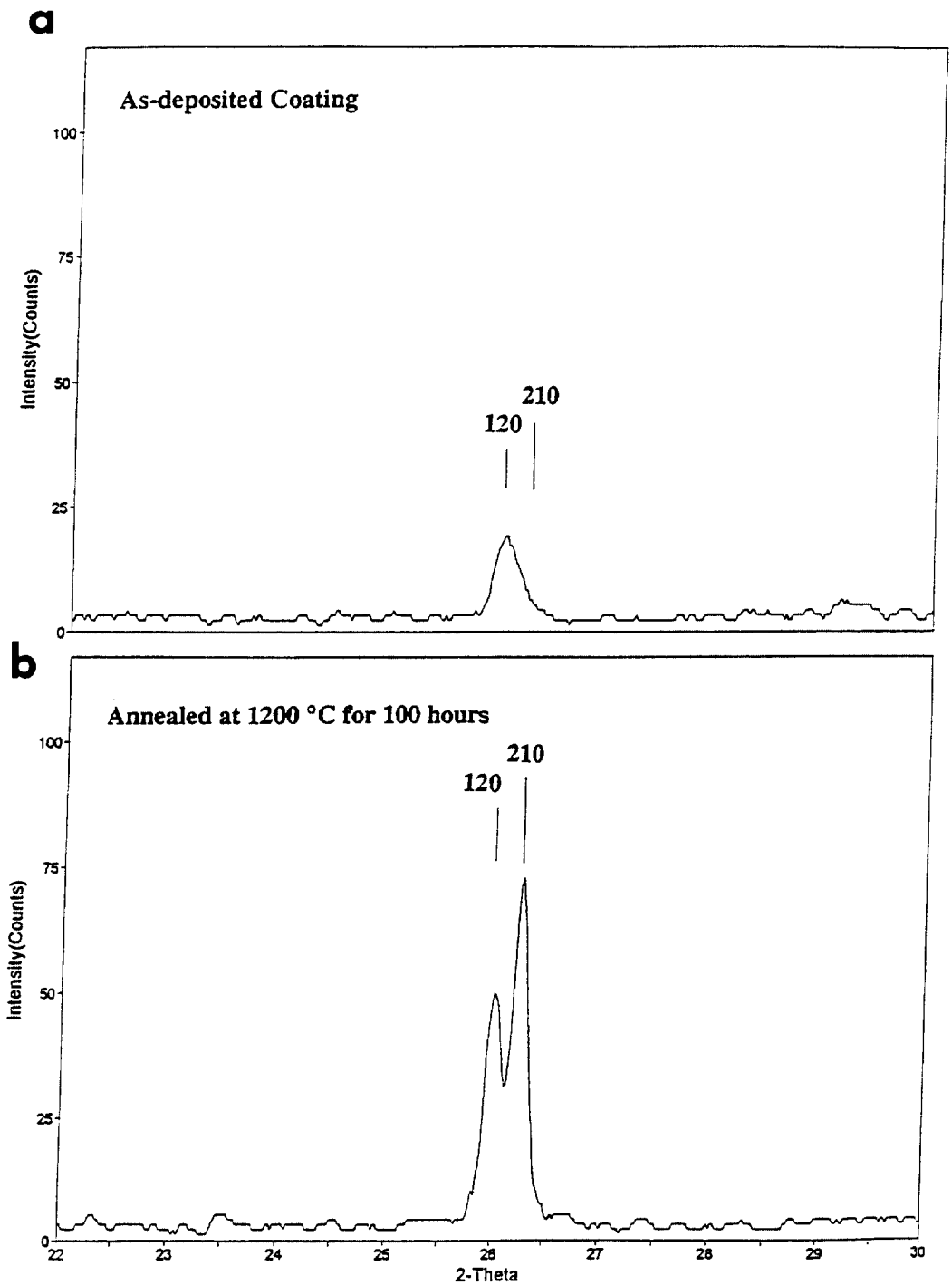

Fig. 12. (a) XRD plot of as-deposited mullite coatings, showing no splitting of the (120)/(210) peaks, implying a tetragonal structure. (b) On annealing for 100 h at 1200°C the structure transforms to orthorhombic, as shown by a clear splitting of the (120)/(210) peaks.

Materials Program with Martin Marietta Energy Systems, Inc.

References

[1] Jacobson NS. J Am Ceram Soc 1993;76(1):3
[2] Jacobson NS, Lee KN, Yoshio Y. J Am Ceram Soc 1996;79(8):2161
[3] Lee KN, Jacobson NS, Miller RA. MRS Bull 1994;19(10):35
[4] Sarin VK. Coat Technol 1995;73:23
[5] Mulpuri RP, Sarin VK. J Mater Res 1996;11(6):1315
[6] Doppalapudi D. Structure and phase transformations in CVD mullite coatings. MS Thesis, Boston University, 1995.
[7] Sundaresan S, Askay IA. J Am Ceram Soc 1991;73(10):2388
[8] Auger ML, Sarin VK. Surf Coat Technol 1997;94–95:46
[9] Doppalapudi D, Basu SN. Mater Sci Eng 1997;A231:48
[10] Cameron WE. Am Mineral 1977;62:747
[11] Smith DGW, McConnell JDC. Miner Mag 1966;35:810